

## **Mantle helium reveals Southern Ocean hydrothermal venting**

Gisela Winckler<sup>1,2,\*</sup>, Robert Newton<sup>1</sup>, Peter Schlosser<sup>1,2,3</sup> and Timothy J Crone<sup>1</sup>

<sup>1</sup> *Lamont-Doherty Earth Observatory, Columbia University, Palisades, NY 10964*

<sup>2</sup> *Department of Earth and Environmental Sciences, Columbia University, New York, NY 10027*

<sup>3</sup> *Department of Earth and Environmental Engineering, Columbia University, New York, NY 10027*

\*Corresponding Author: Gisela Winckler

Lamont-Doherty Earth Observatory, 61 Route 9W, Palisades NY 10964

Phone: (845) 365 8756

Fax: (845) 365 8155

Email: [winckler@ldeo.columbia.edu](mailto:winckler@ldeo.columbia.edu)

1 **Abstract**

2 Hydrothermal venting along the global mid-ocean ridge system plays a major role in  
3 cycling elements and energy between the Earth's interior and surface. We use the  
4 distribution of helium isotopes along an oceanic transect at 67°S to identify previously  
5 unobserved hydrothermal activity in the Pacific sector of the Southern Ocean. Combining  
6 the geochemical information provided by the helium isotope anomaly with independent  
7 hydrographic information from the Southern Ocean, we trace the source of the  
8 hydrothermal input to the Pacific Antarctic Ridge south of 55°S, one of the major global  
9 mid-ocean ridge systems, which has until now been a 'blank spot' on the global map of  
10 hydrothermal venting. We identify three complete ridge segments, a portion of a fourth  
11 segment and two isolated locations on the Pacific Antarctic Ridge between 145°W and  
12 175°W (representing ~540 km of ridge in total) as the potential source of the newly  
13 observed plume.

14

14 **1. Introduction**

15 The observation of submarine hydrothermal vents along the global mid-ocean ridge  
16 system in the late 1970s [*Corliss, et al.*, 1979; *Spiess, et al.*, 1980] remains among the  
17 most important discoveries in modern earth science [*German and Von Damm*, 2003].  
18 Hydrothermal circulation impacts global cycling of elements [*Elderfield and Schultz*,  
19 1996], including economically valuable minerals, and provides extreme ecological niches  
20 that host unique chemosynthetic fauna [*Lutz and Kennish*, 1993; *Van Dover, et al.*, 2002].  
21 Additionally, trace elements emanating from hydrothermal vents such as  $^3\text{He}$  are  
22 uniquely suited for mapping deep ocean circulation and mixing [*Lupton*, 1998; *Lupton*  
23 *and Craig*, 1981; *Naveira Garabato, et al.*, 2007].  
24 During 30 years of seafloor exploration, more than 220 active vent sites have been  
25 identified along the  $\sim 58,000$  km of global mid-ocean ridge crests, over half of them  
26 along spreading ridges in the eastern Pacific Ocean [*Baker and German*, 2004]. However,  
27 no active venting has been observed south of  $38^\circ\text{S}$  in the Pacific Ocean or the Pacific  
28 Sector of the Southern Ocean along the Pacific Antarctic Ridge, which traverses 7000 km  
29 from the Chile Triple Junction through the Southern Ocean to the Macquarie Triple  
30 Junction south of New Zealand.  
31 Here, we use water column measurements of helium isotopes to identify and map a novel  
32 source of hydrothermal venting into the Pacific sector of the Southern Ocean.  
33 Hydrothermal fluids are enriched by about a factor of 10 in the light isotope of helium,  
34  $^3\text{He}$ , relative to the atmospheric helium ratio [e.g., *Jenkins, et al.*, 1978; *Lupton and*  
35 *Craig*, 1981]. The source of this  $^3\text{He}$  excess is mantle  $^3\text{He}$  trapped in the Earth's interior  
36 during its formation and released mainly through volcanic processes at mid-ocean ridges

37 [Lupton, 1983; Welhan and Craig, 1979]. Ascending from the seafloor, the hydrothermal  
38 fluids entrain ambient seawater, rise until becoming neutrally buoyant and form  $^3\text{He}$  –  
39 tagged hydrothermal plumes [Helfrich and Speer, 1995].  
40 Vertical mixing in the ocean is inhibited by density stratification. Thus, dispersion of  
41 trace element signals strongly follows isopycnal surfaces along which the energy required  
42 for transport is minimized. These surfaces of maximal dispersion have been labeled by a  
43 system of neutral density coordinates ( $\gamma_n$ ) [Jackett and McDougall, 1997], and are nearly  
44 horizontal over most of the ocean. They carry conservative tracers over long distances  
45 with relatively little diapycnal dispersion. Because it is biologically and chemically inert  
46 and has a high signal-to-noise ratio,  $^3\text{He}$  is uniquely suited as a marker of the neutral  
47 density layer into which the hydrothermal signal is injected. Conversely, the presence of  
48 a  $^3\text{He}$  plume can be used to identify and trace hydrothermal activity in the deep ocean  
49 over thousands of kilometers.

## 50 **2. Methods**

51 Helium isotope data used in this study were collected as part of the WOCE hydrographic  
52 program and are available from the CLIVAR (Climate Variability and Predictability) &  
53 Carbon Hydrographic Data Office (<http://whpo.ucsd.edu>). Sample collection followed  
54 standard WOCE protocols, with helium samples being drawn immediately after opening  
55 the seals of the 10-liter Niskin bottles in a multi-bottle sampling rosette. Samples were  
56 stored in copper tubes for laboratory analysis, with tritium measured on all samples to  
57 correct for  $^3\text{He}$  ingrowth during storage. P16S samples shallower than about 1500 m  
58 were measured at the Woods Hole Oceanographic Institute (PI Jenkins). P16S samples  
59 deeper than about 1500 m were measured at the NOAA Pacific Marine Environmental

60 Laboratory (PI Lupton). S4P samples were measured at Lamont Doherty Earth  
61 Observatory (PI Schlosser). Helium isotope ratios are reported as  $\delta^3\text{He}$ , which is the  
62 percent deviation of the  $^3\text{He}/^4\text{He}$  ratio of the sample ( $R_{\text{sample}}$ ) from that of atmospheric air  
63 ( $R_{\text{air}}$ ), defined as  $\delta^3\text{He} = [R_{\text{sample}}/R_{\text{air}} - 1] * 100$ . All three laboratories report a  $1\sigma$  precision  
64 of approximately 0.2% in  $\delta^3\text{He}$ .

65 The neutral densities along P16S and S4P were calculated from salinity, temperature and  
66 pressure data collected on-board. For locating potential vent sites, the depth of the 28.2  
67 neutral density surface was calculated using the Southern Ocean Database (SODB,  
68 available at <http://woceSOatlas.tamu.edu> [*Orsi and Whitworth III, 2005*]), which is a  
69 compilation of hydrographic data from approximately 93,000 stations south of 25°S. The  
70 algorithms of Jackett and McDougall (1997) were applied to the salinity, temperature,  
71 pressure, and position of the station data to calculate the neutral density. Neutral density  
72 surface depths were interpolated linearly in the vertical to the 28.2 surface and, using a  
73 cubic spline, in the horizontal to a 1°-grid for comparison with the TBASE bathymetry  
74 from the National Geophysical Data Center [*Row and Hastings, 1999*].

75

### 76 **3. Results and Discussion**

77 We evaluate the distribution of  $^3\text{He}$  along two ocean transects from the WOCE  
78 hydrographic program [*Talley, 2007*]: the meridional WOCE line P16S at 150°W and the  
79 zonal transect S4P at 67°S in the Pacific sector of the Southern Ocean (Figure 1a).

80 The meridional transect along WOCE line P16S at 150°W displays the well-known major  
81 South Pacific helium plume [*Lupton, 1998; Lupton and Craig, 1981*] with  $\delta^3\text{He}$  values of

82 up to approximately 35%. The helium plume emanating from the Southern East Pacific  
83 Rise (S-EPR) is well-mapped [Lupton, 1998; Takahata, *et al.*, 2005] and its primary  
84 source vent fields have been investigated [Auzende, *et al.*, 1996; Baker, *et al.*, 2002;  
85 Urabe, *et al.*, 1995]. The S-EPR helium plume is centered on the  $\gamma_n=27.9$  surface  
86 (Figure 1b). This density surface, and the center of the S-EPR plume, can be identified at  
87 about 2500 m water depth throughout most of the South Pacific Ocean. It rises sharply  
88 south of 45°S as a result of large-scale wind-driven upwelling in the Antarctic  
89 Circumpolar Current (ACC).

90 Along transect S4P at 67°S (Figure 1c), the  $\gamma_n=27.9$  surface has shoaled to between 50  
91 and 700 m depth. It carries a remnant  $^3\text{He}$  anomaly that can be traced back to the S-EPR  
92 plume. However, at this latitude, wind-driven upwelling in the ACC has vented most of  
93 the  $^3\text{He}$  from the S-EPR plume to the atmosphere. Neutral density surfaces less than  
94 about 27.8 have outcropped north of the S4P transect, and even those in the center of the  
95 plume have been exposed to the winter mixed layer which has dramatically reduced peak  
96  $\delta^3\text{He}$  values on the  $\gamma_n=27.9$  surface at this latitude.

97 In the same transect a second deeper  $\delta^3\text{He}$  maximum with  $\delta^3\text{He}$  values of about 11% is  
98 clearly visible (Figure 1c). While exhibiting a smaller anomaly than the main S-EPR  
99 plume to the North, the deep plume is present at all stations of the S4P transect. It follows  
100 the contours of the  $\gamma_n=28.2$  surface across the entire 4500 km transect and represents the  
101 most distinguished feature in the  $^3\text{He}$  distribution over much of the Pacific sector of the  
102 Southern Ocean. The  $\gamma_n=28.2$  surface, and the  $\delta^3\text{He}$  maximum, lie at about 1500 m water  
103 depth in the west and tilt downward to about 3000 m at the eastern end of the transect,

104 which is consistent with the pattern of on- and off-shore currents along the Antarctic  
105 continental slope. At all longitudes, the  $\delta^3\text{He}$  maximum sits well below the remnant  
106 signal of the S-EPR plume. This implies that the Southern Ocean plume is fed from a  
107 hydrothermal source distinct from the main S-EPR plume. This source must interact with  
108 the very dense  $\gamma_n=28.2$  water mass that is characteristic of the region along the Antarctic  
109 continental slope, unequivocally locating the source to be in the Pacific sector of the  
110 Southern Ocean. The different magnitude of the  $\delta^3\text{He}$  anomaly between the SO plume  
111 and the S-EPR plume reflects the combined effect of the strength of the hydrothermal  
112 flux, which is thought to be a function of the local spreading rate [Farley, *et al.*, 1995]  
113 and the mean residence time in the South Pacific basin or the Southern Ocean,  
114 respectively [Schlosser and Winckler, 2002].

115 What is the source of the Southern Ocean plume? To obtain a three-dimensional  
116 perspective of the possible source regions of the Southern Ocean plume, we used  
117 hydrographic data from the Southern Ocean Database [Orsi and Whitworth III, 2005] to  
118 map the depth of the  $\gamma_n=28.2$  neutral density surface, which carries the  $^3\text{He}$  maximum  
119 marking the SO plume onto the bathymetry of the Southern Ocean. In the eastern Pacific  
120 sector of the Southern Ocean, east of about  $145^\circ\text{W}$ , the surface does not extend to the  
121 crest of the Pacific Antarctic Ridge, dead-ending on its southern flank, which excludes  
122 this section of the ridge as a source of the Southern Ocean plume. West of  $145^\circ\text{W}$  the  
123 surface crosses the Pacific Antarctic Ridge close to the seafloor. Along the meridional  
124 transect P16S at  $150^\circ\text{W}$ , for example, the  $\gamma_n=28.2$  surface terminates at about  $55^\circ\text{S}$  on the  
125 northern flank of the ridge (Figure 1b). The Southern Ocean plume is found at this  
126 transect over the Pacific Antarctic Ridge at the southernmost two stations (Figure 1b).

127 The section of the PAR west of 175°W consists almost entirely of fracture zones.  
128 Because fracture zones typically have low magma budgets [*Cormier, et al.*, 1984], and  
129 any helium anomaly would likely originate from a hydrothermal system driven by  
130 magmatic heating, the fracture zone-dominated PAR west of 175° is an unlikely source  
131 of the observed helium plume. Thus, we focus our analysis on the spreading center  
132 between 175°W (Erebus Fracture Zone) and 145°W (Udintsev Fracture Zone), identified  
133 in Figure 1a as red dashed line.

134 As revealed by satellite gravity data and detailed swath bathymetry, the axial morphology  
135 of the PAR between 175°W in this region changes from a rift valley in the western part  
136 (from 175°W to ~ 157°W) to an axial dome in the eastern part (157°W and 145°W) of the  
137 section, reflecting the along-axis increase in spreading rate from slow to fast [*Géli, et al.*,  
138 1997; *Ondréas, et al.*, 2001]. As is typical for slow spreading centers, the western part of  
139 the section is characterized by a rough sea floor with many well-marked fracture zones.  
140 The eastern part of the section is smooth sea floor, typical for fast spreading centers  
141 [*Géli, et al.*, 1997].

142 To localize potential source regions along the Pacific-Antarctic Ridge, we contoured the  
143 neutral density distribution along the ridge crest of the PAR between 175°W and 145°W  
144 (Figure 2) and identified the height of the  $\gamma_n = 28.2$  surface above the ridge (black line).  
145 Because chronic hydrothermal plumes typically rise about 250-300 meters into the water  
146 column before becoming neutrally buoyant and spreading laterally along isopycnals  
147 [*Baker and German, 2004*], we mapped all areas along the PAR section where the  
148  $\gamma_n=28.2$  surface clears the ridge crest by less than 300 m (Figure 3). This is a somewhat  
149 conservative approach which accounts for the possibility that the venting might occur



150 below the ridge crest, for example on a side wall of the rift valley, or that the  
151 hydrothermal fluid rises to less than 300 m. The candidate source locations are  
152 constrained to three complete ridge segments, a portion of a fourth segment, and two  
153 additional isolated locations. In the transition zone between the slow and fast spreading  
154 parts of the ridge we identify two potential source candidates, including a ridge segment  
155 between about 170°W and 168°W and a location at about 162°. In the fast spreading part  
156 of the ridge we identify four potential sources: a prominent segment between 151°W and  
157 153°W, two smaller ridge sections at 148°W and 146.5°W, and a location at about  
158 145°W. Overall, our mapping approach allows us to localize the probable venting region  
159 to approximately 540 kilometers of ridge extent constituting less than 30% of the total  
160 ridge length.

161 The finding that the PAR may be hydrothermally active is not unexpected. Hydrothermal  
162 venting is common along the global chain of seafloor volcanoes. However, the factors  
163 influencing their location and extent are not well understood [e.g., *Fisher, 2004; Tolstoy,*  
164 *2009*]. So far, only a small fraction of the global mid-ocean ridge system has been  
165 systematically surveyed for indications of venting. Our approach, combining the  
166 geochemical information provided by the helium isotope anomaly in the water column  
167 with independent hydrographic information from the Southern Ocean Database (SODB)  
168 and sea-floor topographic data allows us to both trace the source of a far-field  
169 hydrothermal plume to the Pacific Antarctic Ridge, one of the major global mid-ocean  
170 ridge systems, and provide locations to focus a future search for venting along the ridge  
171 crest. This information may be valuable to prioritize future exploration of the  
172 hydrothermal venting systems of the Pacific Antarctic Ridge.

173 **4. Conclusions**

174 We document mantle  $^3\text{He}$  and, by inference, hydrothermal activity on the Pacific-  
175 Antarctic Ridge far south in the Southern Ocean. Our results confirm the assumption of  
176  $^3\text{He}$  injection into the Southern Ocean, as postulated by basin inventories and General  
177 Circulation Models [Farley, *et al.*, 1995]. Interestingly, the Southern Ocean Plume seems  
178 to be unique to the Pacific sector; we have not found comparable features along Indian or  
179 Atlantic sector transects. In addition to its intrinsic geochemical significance, the  
180 hydrothermal signal, since it is injected at depth into a particularly dense water mass  
181 primarily present south of the Pacific Antarctic Ridge and observable across the width of  
182 the basin, provides a unique signal for tracing abyssal circulation and ventilation  
183 processes south of the ACC, such as the formation of Antarctic Bottom Water or mixing  
184 across the ACC. This is particularly important because this region is the locus of the  
185 strongest coupling between the atmosphere and abyssal ocean, and has been implicated in  
186 past climatic changes. Understanding its ventilation patterns and timescales is one of the  
187 most pressing problems in modern physical oceanography.

188 **Acknowledgements.** G.W. thanks Trevor Williams for his generous help with GMT. We  
189 thank Helen Ondréas, Celine Cordier and Louis Géli from Ifremer (Brest, France) for  
190 providing the swath bathymetry data from the PANANTARCTIC cruise.

191 **References**

192 Auzende, J. M., et al. (1996), Recent tectonic, magmatic, and hydrothermal activity on  
193 the East Pacific Rise between 17°S and 19°S: Submersible observations, *J. Geophys.*  
194 *Res.*, *101*, 17995-18010

195 Baker, E. T., and C. R. German (2004), On the global distribution of hydrothermal vent  
196 fields, in *Mid-Ocean Ridges - Hydrothermal interactions between the lithosphere*  
197 *and oceans*, edited by C. R. German, et al., American Geophysical Union,  
198 Washington.

199 Baker, E. T., et al. (2002), Hydrothermal venting along earth's fastest spreading center:  
200 East Pacific Rise, 27.5 degrees - 32.3 degrees S, *J. Geophys. Res.*, *107*, 2130,  
201 doi:10.1029/2001JB000651

202 Corliss, J. B., et al. (1979), Submarine thermal springs on the Galapagos Rift *Science*,  
203 *203*, 1073-1082

204 Cormier, M. H., P. S. Detrick, and G. M. Purdy (1984), Anomalously thin crust in  
205 oceanic fracture zones - New seismic constraints from the Kane fracture-zone, *J.*  
206 *Geophys. Res.*, *89*, 249-266

207 Elderfield, H., and A. Schultz (1996), Mid-ocean ridge hydrothermal fluxes and the  
208 chemical composition of the ocean, *Annu. Rev. Earth Planet. Sci.*, *24*, 191-224

209 Farley, K. A., E. Maier-Reimer, P. Schlosser, and W. S. Broecker (1995), Constraints on  
210 mantle <sup>3</sup>He fluxes and deep-sea circulation from an oceanic general circulation  
211 model, *J. Geophys. Res.*, *100*, 3829-3839

212 Fisher, A. T. (2004), Rates of flow and patterns of fluid circulation, in *Hydrogeology of*  
213 *the Oceanic Lithosphere*, edited by E. E. Davis and H. Elderfield, pp. 339-377,  
214 Cambridge University Press, Cambridge.

215 Géli, L., et al. (1997), Evolution of the Pacific-Antarctic Ridge South of the Udintsev  
216 Fracture Zone, *Science*, *278*, 1281-1284

217 German, C. R., and K. L. Von Damm (2003), Hydrothermal Processes, *Treatise*  
218 *Geochem.*, 6, 181-222

219 Helfrich, K. R., and K. G. Speer (1995), Ocean hydrothermal circulation: mesoscale and  
220 basin-scale flow, in *Seafloor Hydrothermal Systems: Physical chemical, biological,*  
221 *and geological interactions*, edited by S. Humphris, et al., pp. 347-356, AGU.

222 Jackett, D. R., and T. J. McDougall (1997), A neutral density variable for the world's  
223 oceans, *J. Phys. Oceanogr.*, 27, 237-263

224 Jenkins, W. J., J. M. Edmond, and J. B. Corliss (1978), Excess  $^3\text{He}$  and  $^4\text{He}$  in Galapagos  
225 hydrothermal waters, *Nature*, 272, 156-158

226 Lupton, J. (1998), Hydrothermal helium plumes in the Pacific Ocean, *J. Geophys. Res.*,  
227 103, 15853-15868

228 Lupton, J. E. (1983), Terrestrial inert gases: Isotope tracer studies and clues to primordial  
229 components in the mantle, *Annu. Rev. Earth Planet. Sci.*, 11, 371-414

230 Lupton, J. E., and H. Craig (1981), A major  $^3\text{He}$  source at 15°S on the East Pacific Rise,  
231 *Science*, 214, 13-18

232 Lutz, R. A., and J. J. Kennish (1993), Ecology of deep-sea hydrothermal communities,  
233 *Rev. Geophys.*, 31, 211-241

234 Naveira Garabato, A. C., D. P. Stevens, A. J. Watson, and W. Roether (2007), Short-  
235 circuiting of the overturning circulation in the Antarctic Circumpolar Current,  
236 *Nature*, 447, 194-197, doi:10.1038/nature05832

237 Ondréas, H., D. Aslanian, L. Géli, and J.-L. Olivet (2001), Variations in axial  
238 morphology, segmentation, and seafloor roughness along the Pacific-Antarctic Ridge  
239 between 56°S and 66°S *J. Geophys. Res.*, 106, 8521-8546

240 Orsi, A. H., and T. Whitworth III (2005), Hydrographic Atlas of the World Ocean  
241 Circulation Experiment (WOCE), in *Volume 1: Southern Ocean*, edited by M.  
242 Sparrow, et al., International WOCE Project Office, Southampton, UK.

243 Row, L. W. I., and D. Hastings (1999), TBASE/TerrainBase Global Terrain Model  
244 *National Geophysical Data Center-A for Solid Earth Geophysics Boulder, Colorado,*  
245 *USA*, <http://www.ngdc.noaa.gov/mgg/gravity/1999/data/global/tbase/>

246 Schlosser, P., and G. Winckler (2002), Noble gases in the ocean and ocean floor, in  
247 *Noble gases in geochemistry and cosmochemistry*, edited by R. Wieler, et al., pp.  
248 701-730, *Reviews in Mineralogy and Geochemistry*.

249 Spiess, F. N., et al. (1980), East Pacific Rise: hot springs and geophysical experiments,  
250 *Science*, 207, 1421-1433

251 Takahata, N., M. Agarwal, M. Nishizawa, K. Shirai, Y. Inoue, and Y. Sano (2005),  
252 Helium-3 plume over the East Pacific Rise at 25°S, *Geophys. Res. Lett.*, 32, L11608,  
253 doi:10.1029/2005GL023076

254 Talley, L. D. (2007), Hydrographic Atlas of the World Ocean Circulation Experiment  
255 (WOCE), in *Pacific Ocean*, edited by M. Sparrow, et al., International WOCE  
256 Project Office, Southampton, UK.

257 Tolstoy, M. (2009), Where there's smoke there's fire, *Nature Geoscience*, 2, 463-464

258 Urabe, T., et al. (1995), The effect of magmatic activity on hydrothermal venting along  
259 the superfast-spreading East Pacific Rise, *Science*, 269, 1092-1095

260 Van Dover, C. L., C. R. German, K. G. Speer, L. M. Parson, and R. C. Vrijenhoek  
261 (2002), Evolution and biogeography of deep-sea vent and seep invertebrates,  
262 *Science*, 295, 1253-1257

263 Welhan, J. A., and H. Craig (1979), Methane and hydrogen in East Pacific rise  
264 hydrothermal fluids, *Geophys. Res. Lett.*, 6, 829-831

265

## 266 **Figure Legends**

267 **Figure 1:** Helium isotope distribution as marker of hydrothermal activity in the South  
268 Pacific and Southern Ocean. a: Map of the South Pacific with WOCE sections P16S at  
269 150°W and S4P at 67°S (black dots). The red stippled line identifies the potentially active  
270 portion of the Pacific Antarctic Ridge between 175°W to 145°W. b: Vertical section of  
271  $\delta^3\text{He}$  along P16S marking the Southern East Pacific Rise (S-EPR) plume. c: Vertical  
272 section of  $\delta^3\text{He}$  along S4P marking the Southern Ocean (SO) plume.

273 **Figure 2:** Neutral density distribution along the Pacific Antarctic Ridge from 175°W to  
274 145°W (red stippled line in Figure 1a). The thick black line marks the depth of the  
275  $\gamma_n=28.2$  surface that carries the  $^3\text{He}$  anomaly. High resolution swath bathymetry of the  
276 ridge is from *Géli, et al.* [1997]. The blanked areas mark fracture zones. We map  
277 locations where the height of the  $\gamma_n = 28.2$  surface is less than 300 m above the ridge to  
278 identify potential sources of the Southern Ocean plume (Figure 3).

279 **Figure 3:** Map showing the Pacific Antarctic Ridge from 175°W to 145°W (red stippled  
280 line in Figure 1a) with the height of the  $\gamma_n = 28.2$  neutral density surface above the ridge  
281 indicated with colored dots. Locations where the vertical distance between the 28.2  
282 surface and the ridge crest is below 300 m are colored in shades of yellow and red and  
283 indicate potential sources of the Southern Ocean plume. Locations where this surface is  
284 above 300 m height are colored in shades of blue.

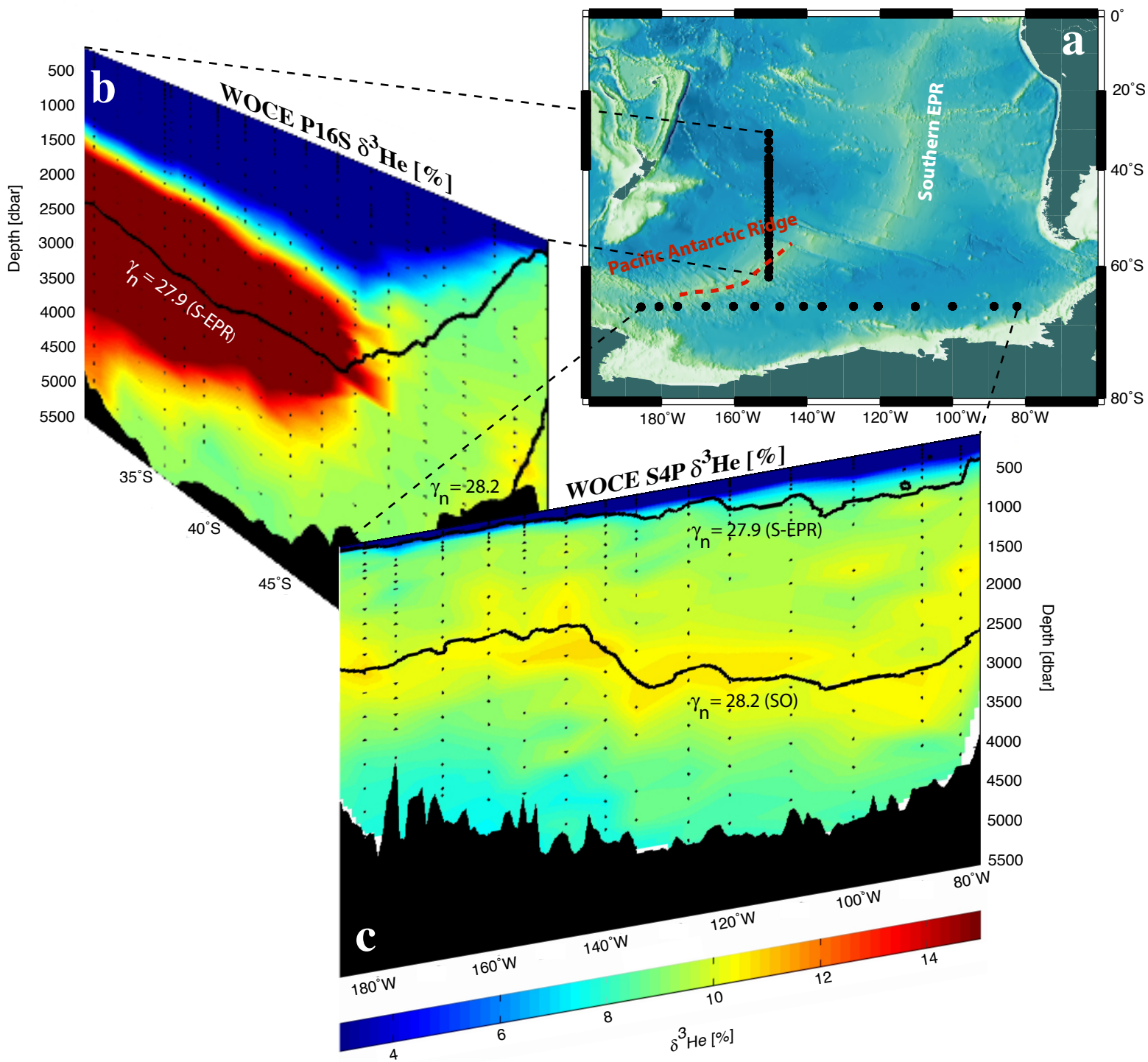


**Figure 1:** Helium isotope distribution as marker of hydrothermal activity in the South Pacific and Pacific sector of the Southern Ocean

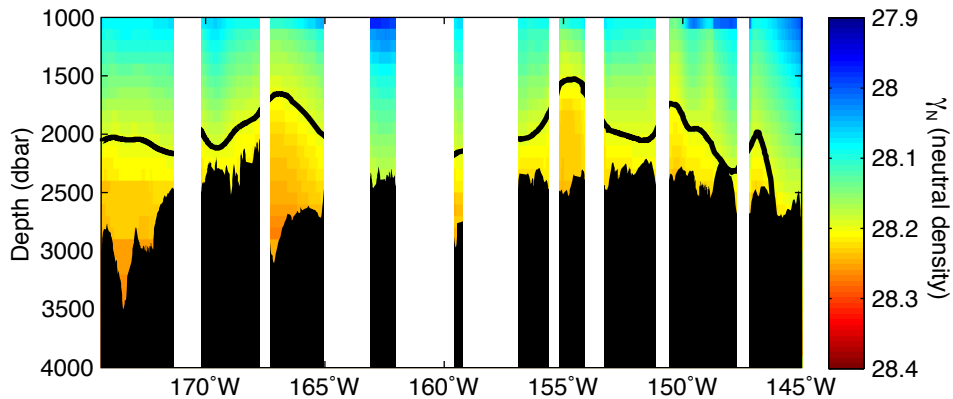


**Figure 2:** Neutral density distribution along the Pacific Antarctic Ridge from 175°W to 145°W (red stippled line in Figure 1a). The thick black line marks the depth of the  $\gamma_n=28.2$  surface that carries the  $^3\text{He}$  anomaly. High resolution swath bathymetry of the ridge is from Géli, et al. [1997]. The blanked areas mark fracture zones. We map locations where the height of the  $\gamma_n = 28.2$  surface is less than 300 m above the ridge to identify potential sources of the Southern Ocean plume (Figure 3).



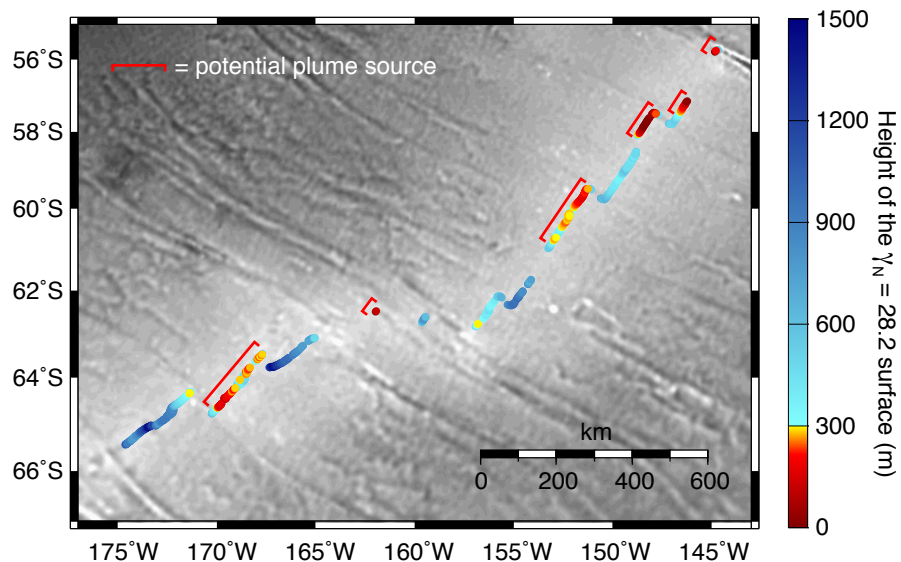


**Figure 3:** Map showing the Pacific Antarctic Ridge from 175°W to 145°W (red stippled line in Figure 1a) with the height of the  $\gamma_n = 28.2$  neutral density surface above the ridge indicated with colored dots. Locations where the vertical distance between the 28.2 surface and the ridge crest is below 300 m are colored in shades of yellow and red and indicate potential sources of the Southern Ocean plume. Locations where this surface is above 300 m height are colored in shades of blue.